

COEFFICIENTS-PRESERVING SAMPLING FOR REINFORCEMENT LEARNING WITH FLOW MATCHING

Feng Wang*, Zihao Yu

CreateAI (<https://www.iamcreate.ai/>)

feng.wff@gmail.com, zi_hao_yu@163.com

ABSTRACT

Reinforcement Learning (RL) has recently emerged as a powerful technique for improving image and video generation in Diffusion and Flow Matching models, specifically for enhancing output quality and alignment with prompts. A critical step for applying online RL methods on Flow Matching is the introduction of stochasticity into the deterministic framework, commonly realized by Stochastic Differential Equation (SDE). Our investigation reveals a significant drawback to this approach: SDE-based sampling introduces pronounced noise artifacts in the generated images, which we found to be detrimental to the reward learning process. A rigorous theoretical analysis traces the origin of this noise to an excess of stochasticity injected during inference. To address this, we draw inspiration from Denoising Diffusion Implicit Models (DDIM) to reformulate the sampling process. Our proposed method, Coefficients-Preserving Sampling (CPS), eliminates these noise artifacts. This leads to more accurate reward modeling, ultimately enabling faster and more stable convergence for reinforcement learning-based optimizers like Flow-GRPO and Dance-GRPO.

1 INTRODUCTION

The paradigm of unsupervised pre-training, followed by supervised fine-tuning and reinforcement learning post-training, has become the new standard for training next-generation deep learning models (Achiam et al. (2023); Ouyang et al. (2022)). Inspired by the application of reinforcement learning in Large Language Models (Gao et al. (2023); Rafailov et al. (2023)), RL algorithms have also been adopted in the image and video generation domains (Black et al. (2023); Miao et al. (2024); Wallace et al. (2024); Dong et al. (2023); Yang et al. (2024)). Recently, a series of algorithms have utilized Group Relative Policy Optimization (GRPO) to optimize for specific rewards (Liu et al. (2025); Xue et al. (2025)), achieving impressive results in metrics such as aesthetics (Kirstain et al. (2023); Wu et al. (2023)), instruction following (Hessel et al. (2021)), and image-to-video consistency (Jiang et al. (2024)).

The standard RL loop comprises three stages: sampling, reward and advantage computation, and policy optimization. A crucial requirement of the sampling stage is to generate a group of highly diverse samples for each prompt. To this end, methods such as Flow-GRPO (Liu et al. (2025)) and Dance-GRPO (Xue et al. (2025)) introduce stochasticity by reformulating the deterministic Ordinary Differential Equation (ODE) of the generative process as a Stochastic Differential Equation (SDE). However, we identify that during training, this SDE-based sampling produces outputs always corrupted by conspicuous noise artifacts (see Figure 1). The rewards, which guide the policy updates, are computed from these noisy samples. Consequently, reward models designed to assess aesthetic quality or human preference often assign inaccurate scores and rankings, thereby misleading the learning process.

To resolve this, we thoroughly investigated the SDE sampling mechanism. Our analysis revealed that the SDE formulation injects greater amount of noise than the original ODE. As the original ODE scheduler is retained, this excess noise accumulates, leading to a non-zero final noise level and visibly noisy outputs. Fundamentally, this problem stems from a mismatch between the SDE’s

*Corresponding author.



Figure 1: The images sampled by Flow-SDE exhibit severe noise, and the noise magnitude increases with higher sampling noise parameters. In contrast, our Coefficients-Preserving Sampling (CPS) algorithm produces noise-free images regardless of the noise level. Notably, these images will be fed into a reward model, and the noisy images may lead to inaccurate rewards.

score function term and the noise level introduced by the Wiener process. Inspired by DDIM (Song et al. (2021a)), we reformulated the noise injection method during sampling to ensure that at every timestep, the noise level of the latent variable remains consistent with the scheduler.

We empirically validated our enhanced algorithm on multiple baseline models and with a variety of reward functions. The results confirm that for reward models predicated on aesthetics and human preferences, our method consistently demonstrates superior convergence rates and achieves higher terminal reward values. For detection-based reward models, our method achieves faster convergence rates with a similar final reward.

2 RELATED WORK

2.1 ALIGNMENT FOR LARGE LANGUAGE MODELS

With the advent of Large Language Models (LLMs)(Brown et al. (2020); Achiam et al. (2023)), Reinforcement Learning (RL) has garnered renewed attention. The Reinforcement Learning from Human Feedback (RLHF) framework(Ouyang et al. (2022); Gao et al. (2023)), for instance, trains a reward model using human preference data, which in turn fine-tunes the LLM to better align with human expectations. As an alternative to computationally intensive policy gradient methods, Direct Preference Optimization (DPO)(Rafailov et al. (2023)) provides a more streamlined approach that directly trains the model on human preference data. More recently, advanced techniques have been applied to enhance multi-step reasoning. For example, OpenAI-o1 utilizes Proximal Policy Optimization (PPO)(Schulman et al. (2017)) and DeepSeek-R1 employs Group Relative Policy Optimization (GRPO)(Shao et al. (2024)), both using verifiable rewards to improve the models' capacity for extended reasoning via chain-of-thought.

2.2 ALIGNMENT FOR DIFFUSION

Analogous to autoregressive LLMs, both Diffusion(Ho et al. (2020); Song et al. (2021a;b)) and Flow Matching(Lipman et al. (2022); Liu et al. (2022)) models usually construct their outputs via a multi-step sampling process. They can therefore be aligned using similar RL-based techniques. As such, diffusion models are compatible with optimization algorithms including DPO(Wallace et al.

(2024); Dong et al. (2023); Yang et al. (2024)), PPO-style policy gradients(Black et al. (2023); Miao et al. (2024); Zhao et al. (2025)), and GRPO(Liu et al. (2025); Xue et al. (2025)). However, unlike token-based models that involve discrete selection steps, the absence of quantization in the diffusion process permits an alternative training paradigm: the direct backpropagation of gradients through the full sampling trajectory Xu et al. (2023).

2.3 DIFFUSION SAMPLER

Efficient sampling is a critical research area for diffusion models. Samplers can be broadly categorized by the numerical methods they adapt. Foundational approaches like DDPM (Ho et al. (2020)) established the paradigm but were slow. Denoising Diffusion Implicit Models (Song et al. (2021a)) provided one of the first major speed improvements by formulating a deterministic sampling process. Subsequently, a significant body of work has focused on applying and adapting sophisticated ordinary differential equation (ODE) solvers. For instance, first-order methods like the Euler solver (Song et al. (2021b)) offer speed at the cost of accuracy, while second-order methods like Heun’s method (Karras et al. (2022)) provide a better balance. High-order solvers, such as DPM-Solver (Lu et al. (2022; 2025)), have become popular for their dramatic reduction in required sampling steps. Another effective approach is the predictor-corrector framework, exemplified by UniPC (Zhao et al. (2023)), which unifies these two steps to achieve robust and high-quality generation with minimal function evaluations.

3 PRELIMINARIES

In this section, we introduce the formulations of Flow Matching, Flow-GRPO, Dance-GRPO and DDIM. They will be the basic knowledge for our proposed algorithm.

Flow Matching Assume that $\mathbf{x}_0 \sim X_0$ is sampled from the data distribution and $\mathbf{x}_1 \sim X_1$ is a gaussian noise sample, Rectified Flow (Liu et al. (2022)) interpolates noised sample \mathbf{x}_t as,

$$\mathbf{x}_t = (1 - t)\mathbf{x}_0 + t\mathbf{x}_1, \quad (1)$$

where $t \in [0, 1]$ is the *noise level*. Then a neural network is trained to regress the velocity $\mathbf{v} = \mathbf{x}_1 - \mathbf{x}_0$. Finally, Flow Matching methods use a deterministic ODE for the forward process:

$$d\mathbf{x}_t = \hat{\mathbf{v}}_\theta(\mathbf{x}_t, t)dt, \quad (2)$$

where $\hat{\mathbf{v}}_\theta(\mathbf{x}_t, t)$ is the estimated velocity. The $\hat{\cdot}$ denotes that the value is estimated in the following article.

Flow-GRPO and Dance-GRPO Reinforcement Learning relies on stochastic sampling to generate diverse samples. Flow-GRPO (Liu et al. (2025)) and Dance-GRPO (Xue et al. (2025)) introduce randomness into Flow Matching by converting the deterministic Flow-ODE into Flow-SDE,

$$d\mathbf{x}_t = [\mathbf{v}_\theta(\mathbf{x}_t, t) + \frac{\sigma_t^2}{2t}(\mathbf{x}_t + (1 - t)\hat{\mathbf{v}}_\theta(\mathbf{x}_t, t))]dt + \sigma_t\sqrt{dt}\epsilon, \quad (3)$$

where $\epsilon \sim \mathcal{N}(0, \mathbf{I})$ is a newly sampled gaussian noise, $\sigma_t = \eta\sqrt{\frac{t}{1-t}}$ for Flow-GRPO and $\sigma_t = \eta$ for Dance-GRPO.

After sampling a group of G diverse images $\{\mathbf{x}_0^i\}_{i=1}^G$, the rewards $R(\mathbf{x}_0^i)$ are transformed to advantages by,

$$\hat{A}_t^i = \frac{R(\mathbf{x}_0^i) - \text{mean}(\{R(\mathbf{x}_0^i)\}_{i=1}^G)}{\text{std}(\{R(\mathbf{x}_0^i)\}_{i=1}^G)}. \quad (4)$$

Then GRPO (Shao et al. (2024)) optimizes the policy model by maximizing the following objective,

$$\mathcal{L}(\theta) = \mathbb{E}_{\mathbf{c} \sim \mathcal{C}, \{\mathbf{x}^i\}_{i=1}^G \sim \pi_{\theta_{\text{old}}}(\cdot|\mathbf{c})} \frac{1}{G} \sum_{i=1}^G \frac{1}{T} \sum_{t=0}^{T-1} (\min(r_t^i(\theta)\hat{A}_t^i, \text{clip}(r_t^i(\theta), 1 - \epsilon, 1 + \epsilon)\hat{A}_t^i)), \quad (5)$$

where $r_t^i(\theta) = \frac{p_\theta(\mathbf{x}_{t-1}^i|\mathbf{x}_t^i)}{p_{\theta_{\text{old}}}(\mathbf{x}_{t-1}^i|\mathbf{x}_t^i)}$. Here we omit the KL loss term due to space limit.

DDPM and DDIM Sampling SDE is not the only way to inject stochasticity. In the DDIM sampling procedure,

$$\mathbf{x}_{t-1} = \underbrace{\sqrt{\alpha_{t-1}} \left(\frac{\mathbf{x}_t - \sqrt{1 - \alpha_t} \epsilon_{\theta}^{(t)}(\mathbf{x}_t)}{\sqrt{\alpha_t}} \right)}_{\text{predicted } \mathbf{x}_0} + \underbrace{\sqrt{1 - \alpha_{t-1} - \sigma_t^2}}_{\text{predicted noise}} \cdot \underbrace{\epsilon_{\theta}^{(t)}(\mathbf{x}_t)}_{\text{predicted noise}} + \underbrace{\sigma_t \epsilon_t}_{\text{random noise}}, \quad (6)$$

where $\epsilon_t \sim \mathcal{N}(\mathbf{0}, \mathbf{I})$ is standard Gaussian noise independent of $\epsilon_{\theta}^{(t)}(\mathbf{x}_t)$. For other notations, please refer to the DDIM paper (Song et al. (2021a)). When $\sigma_t = \sqrt{(1 - \alpha_{t-1})/(1 - \alpha_t)} \sqrt{1 - \alpha_t/\alpha_{t-1}}$, the forward process becomes Markovian, and the generative process becomes a DDPM. When $\sigma_t = 0$, the resulting model becomes an implicit probabilistic model (DDIM). For other σ_t , we call it DDIM with stochasticity.

The relationship between DDIM and DDPM is similar to that between ODE and SDE: DDIM and ODE are deterministic, while DDPM and SDE inject stochasticity into their counterparts.

4 ANALYSIS AND METHODS

In this section, we first introduce the concept of coefficients-preserving sampling (CPS). Then we prove that the SDE used in Flow-GRPO and Dance-GPRO cannot match the requirements of CPS. Finally, we provide an alternative to SDE to inject stochasticity for flow matching.

4.1 COEFFICIENTS-PRESERVING SAMPLING

During the sampling process of flow matching, we can get the predicted sample $\hat{\mathbf{x}}_0$ and noise $\hat{\mathbf{x}}_1$ by,

$$\hat{\mathbf{x}}_0 = \mathbf{x}_t - t\hat{\mathbf{v}}, \quad \hat{\mathbf{x}}_1 = \mathbf{x}_t + (1 - t)\hat{\mathbf{v}}. \quad (7)$$

Referring to Equation 6 and 7, we can rewrite the sampling function as,

$$\begin{aligned} \hat{\mathbf{x}}_{t-\Delta t} &= \mathbf{x}_t - \hat{\mathbf{v}}_{\theta}(\mathbf{x}_t, t)\Delta t \\ &= (1 - (t - \Delta t)) \underbrace{(\mathbf{x}_t - t\hat{\mathbf{v}}_{\theta}(\mathbf{x}_t, t))}_{\text{predicted } \hat{\mathbf{x}}_0} + (t - \Delta t) \underbrace{(\mathbf{x}_t + (1 - t)\hat{\mathbf{v}}_{\theta}(\mathbf{x}_t, t))}_{\text{predicted } \hat{\mathbf{x}}_1} \\ &= \underbrace{(1 - (t - \Delta t))}_{\text{coefficient of sample}} \hat{\mathbf{x}}_0 + \underbrace{(t - \Delta t)}_{\text{coefficient of noise}} \hat{\mathbf{x}}_1, \end{aligned} \quad (8)$$

which is also a linear interpolation between the *predicted* sample $\hat{\mathbf{x}}_0$ and *predicted* noise $\hat{\mathbf{x}}_1$. This equation reveals that the sum of the coefficients for the sample and the noise is always 1, whether for training or inference. If this condition is not satisfied, the out-of-distribution input to the neural network will potentially yield an incorrect velocity field.

Furthermore, the sampling process usually utilizes a scheduler that strictly defines the target t for each step. Denoising too much or too little at any timestep will distort the final generated image. Based on the preceding analysis, we define coefficients-preserving sampling as follows:

Definition 1 (Coefficients-Preserving Sampling) A sampling process is considered to be *coefficients preserving* if it satisfies the following two conditions:

1. The coefficient of the sample should be strictly allocated by the scheduler for all timesteps.
2. The total noise level, defined as the standard deviation of a single multivariate noise or the sum of multiple independent noises, must align with the scheduler for all timesteps.

DDIM sampling is Coefficients-Preserving: From Equation 6, there are two independent noise terms, whose coefficients are $\sqrt{1 - \alpha_{t-1} - \sigma_t^2}$ and σ_t , so the final noise level is $\sqrt{1 - \alpha_{t-1}}$. The sample coefficient is $\sqrt{\alpha_{t-1}}$, so the squared sum of the two coefficients is 1. These two coefficients exactly match the DDIM schedule, whatever σ_t is. Thus, we say the sampling procedure of DDIM is Coefficients-Preserving Sampling.

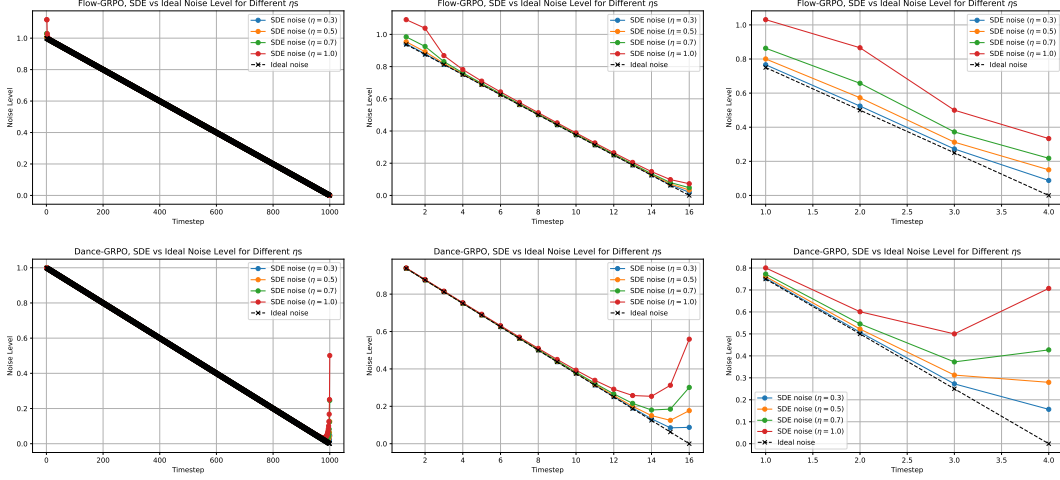


Figure 2: The ideal and SDE noise level for Flow-GRPO and Dance-GRPO with 1000, 16, and 4 sampling steps. Except for the numerical problem around $t = 0$ and $t = 1$, the error of the noise level increases as the sampling step decreases.

4.2 FLOW-SDE IS NOT COEFFICIENTS-PRESERVING SAMPLING

Recall Equation 3 and rewrite it into the form of Equation 6,

$$\begin{aligned}
 \mathbf{x}_{t-\Delta t} &= \mathbf{x}_t - [\hat{\mathbf{v}}_\theta(\mathbf{x}_t, t) + \underbrace{\frac{\sigma_t^2}{2t} (\mathbf{x}_t + (1-t)\hat{\mathbf{v}}_\theta(\mathbf{x}_t, t))}_{\text{predicted } \hat{\mathbf{x}}_1}] \Delta t + \sigma_t \sqrt{\Delta t} \epsilon \\
 &= \underbrace{\mathbf{x}_t - \hat{\mathbf{v}}_\theta(\mathbf{x}_t, t) \Delta t}_{\text{Equation 8}} - \frac{\sigma_t^2 \Delta t}{2t} \hat{\mathbf{x}}_1 + \sigma_t \sqrt{\Delta t} \epsilon \\
 &= (1 - (t - \Delta t)) \hat{\mathbf{x}}_0 + (t - \Delta t - \frac{\sigma_t^2 \Delta t}{2t}) \hat{\mathbf{x}}_1 + \sigma_t \sqrt{\Delta t} \epsilon.
 \end{aligned} \tag{9}$$

From the above equation, we can infer that the total noise level,

$$\begin{aligned}
 \sigma_{total} &= \sqrt{(t - \Delta t - \frac{\sigma_t^2 \Delta t}{2t})^2 + \sigma_t^2 \Delta t} \\
 &= \sqrt{(t - \Delta t)^2 - \frac{\sigma_t^2 \Delta t}{t} (t - \Delta t) + (\frac{\sigma_t^2 \Delta t}{2t})^2 + \sigma_t^2 \Delta t} \\
 &= \sqrt{(t - \Delta t)^2 + \frac{(\sigma_t \Delta t)^2}{t} + (\frac{\sigma_t^2 \Delta t}{2t})^2} \\
 &\geq t - \Delta t,
 \end{aligned} \tag{10}$$

where the equality holds only if $\sigma_t = 0$, which means no stochasticity. Thus, Flow-SDE cannot satisfy the second condition of CPS. At each timestep t , it mixes a higher level of noise into the latent variable $\mathbf{x}_{t-\Delta t}$, which would cause a wrong velocity direction, and the final sampled image would be noisy as shown in Figure 1.

In Figure 2, we plot the noise level for both Flow-GRPO and Dance-GRPO. As we can see, the noise level mismatch problem is severe for both of them. Moreover, because of the $\frac{\sigma_t^2 \Delta t}{2t}$ term in Equation 9, the error around $t = 0$ is large for Dance-GRPO ($\sigma_t = \eta$). For Flow-GRPO, $\sigma_t = \eta \sqrt{\frac{t}{1-t}}$, the noise level is inaccurate around $t = 1$. The problem becomes even worse when the sampling step is low, e.g. 4 steps for FLUX.1-schnell.

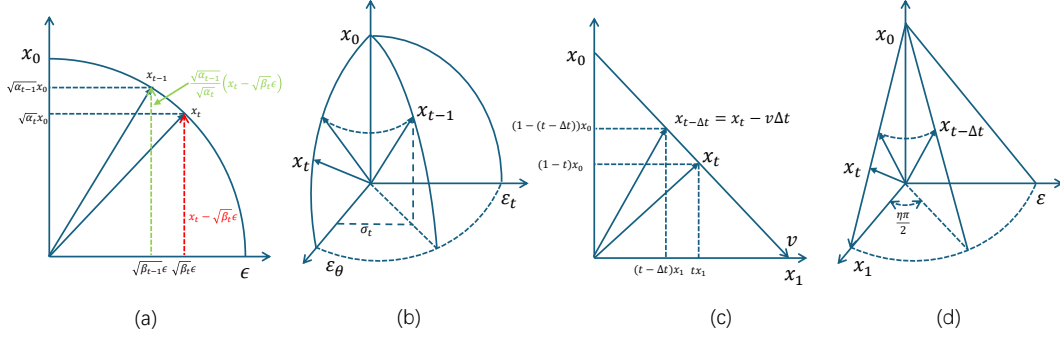


Figure 3: **(a)**: DDIM deterministic sampling process. Note that ϵ is a random Gaussian noise, which is almost orthogonal to the sample x_0 . Since $\sqrt{\alpha_t}^2 + \sqrt{\beta_t}^2 = 1$, the trajectory is part of a quarter-circle at each step. **(b)**: DDIM sampling process with stochasticity (Equation 6). ϵ_t is also a random Gaussian noise, which is almost orthogonal to x_0 and ϵ_θ . **(c)**: Flow matching ODE Sampler. The trajectory is a straight line at each step. **(d)**: Our proposed Coefficients-Preserving Sampling (Equation 12). This figure is inspired by Wang (2024).

4.3 OUR SOLUTION

The main problem of Flow-SDE is that the reduced noise level $\frac{\sigma_t^2 \Delta t}{2t}$ cannot match the newly added noise level $\sigma_t \sqrt{\Delta t}$. Noticing that DDPM also injects noise into the DDIM sampling procedure while preserving the noise level (Figure 3.b), we consider referring to DDIM sampling to solve the problem. Assume that the newly added noise has a variance of σ_t^2 , the coefficient of predicted noise should be $\sqrt{(t - \Delta t)^2 - \sigma_t^2}$ to meet the requirement of the second condition of CPS. In this way, the sampling formulation is,

$$x_{t-\Delta t} = (1 - (t - \Delta t)) \hat{x}_0 + \sqrt{(t - \Delta t)^2 - \sigma_t^2} \hat{x}_1 + \sigma_t \epsilon, \quad (11)$$

which has a very similar form to DDIM with stochasticity (Equation 6).

For the noise level σ_t , the maximum value is $t - \Delta t$, or the *sqrt* term would have a negative radicand. To avoid the negative radicand, we propose to set $\sigma_t = (t - \Delta t) \sin(\frac{\eta\pi}{2})$. Then the sampling formulation becomes,

$$x_{t-\Delta t} = (1 - (t - \Delta t)) \hat{x}_0 + (t - \Delta t) \cos(\frac{\eta\pi}{2}) \hat{x}_1 + (t - \Delta t) \sin(\frac{\eta\pi}{2}) \epsilon, \quad (12)$$

where $\eta \in [0, 1]$ controls the stochastic strength. This formulation satisfies the requirement of CPS and has an intuitive geometric interpretation as shown in Figure 3.d. Because our sampling algorithm is based on the CPS, we name it as Flow-CPS.

To train with GRPO, we also need $p_\theta(x_{t-1}^i | x_t^i)$, which is defined as (Liu et al. (2025)),

$$\log p_\theta(x_{t-1}^i | x_t^i) = -\frac{\|x_{t-\Delta t} - \mu_\theta(x_t, t)\|^2}{2\sigma_t^2} - \log \sigma_t - \log \sqrt{2\pi}, \quad (13)$$

where $\mu_\theta(x_t, t) = (1 - (t - \Delta t)) \hat{x}_0 + (t - \Delta t) \cos(\frac{\eta\pi}{2}) \hat{x}_1$. For each step, the $-\log \sigma_t - \log \sqrt{2\pi}$ is a constant value that cancels out in $r_t^i(\theta) = \frac{p_\theta(x_{t-1}^i | x_t^i)}{p_{\theta_{\text{old}}}(x_{t-1}^i | x_t^i)}$. Moreover, we removed the σ_t in the denominator to avoid division by zero in the last timestep. Thus, our definition of log-probability is as simple as,

$$\log p_\theta(x_{t-1}^i | x_t^i) = -\|x_{t-1} - \mu_\theta(x_t, t)\|^2. \quad (14)$$

4.4 DISCUSSION

In Equation 11, we choose not to build a Wiener process as our objective is to incorporate sufficient stochasticity to produce more diverse samples. To create a Wiener process, just replace σ_t with $\sigma_t \sqrt{\Delta t}$,

$$x_{t-\Delta t} = (1 - (t - \Delta t)) \hat{x}_0 + \sqrt{(t - \Delta t)^2 - \sigma_t^2 \Delta t} \hat{x}_1 + \sigma_t \sqrt{\Delta t} \epsilon. \quad (15)$$

We name this sampling function Flow-CPWS, where W denotes the Wiener process.

Inspired by the derivation of VP SDE (Song et al. (2021b)), which uses Taylor expansion for formula derivation, we can also get an approximate SDE from Flow-CPWS. Note that by Taylor expansion, $\sqrt{t^2 - x} = t - \frac{x}{2t} + O(x)$ around $x = 0$, the above equation can be transformed to,

$$\begin{aligned} x_{t-\Delta t} &\approx (1 - (t - \Delta t)) \hat{x}_0 + \left(t - \Delta t - \frac{\sigma_t^2 \Delta t}{2(t - \Delta t)} \right) \hat{x}_1 + \sigma_t \sqrt{\Delta t} \epsilon \\ &\approx (1 - (t - \Delta t)) \hat{x}_0 + \left(t - \Delta t - \frac{\sigma_t^2 \Delta t}{2t} \right) \hat{x}_1 + \sigma_t \sqrt{\Delta t} \epsilon, \end{aligned} \quad (16)$$

which is the same with Flow-SDE (Equation 9). The approximate equality holds when $\Delta t \rightarrow 0^1$. Now we can conclude:

Theorem 1 *Flow-SDE is a first-order Taylor approximation of Flow-CPWS in the limit of $\Delta t \rightarrow 0$, with a noise level error of $\sqrt{\frac{(\sigma_t \Delta t)^2}{t} + (\frac{\sigma_t^2 \Delta t}{2t})^2}$.*

The proof is provided above by Equation 16 and Equation 10.

For traditional diffusion methods, such as DDPM (Ho et al. (2020)), the sampling step is set as 1000, so the condition $\Delta t \rightarrow 0$ is well satisfied. However, for modern diffusion and flow matching samplers (Song et al. (2021a); Lu et al. (2022)), the sampling step is usually less than 20. With some distillation techniques (Song et al. (2023); Yin et al. (2024)), the sampling step can be reduced to 4 or even 1. The condition $\Delta t \rightarrow 0$ no longer holds in these settings. This is the fundamental reason why Flow-SDE produces inaccurate noise levels.

Furthermore, because of the $\frac{1}{t}$ term after Taylor expansion, the approximation error will be huge around $t = 0$ (Figure 2), so it is inaccurate even when the sampling step number is high. We provide an alternative to bypass this issue in Appendix B.

5 EXPERIMENTS

In this section, we will evaluate the performance of Flow-CPS in the circumstance of GRPO-based reward optimization on four reward models, GenEval (Ghosh et al. (2023)), Text Rendering (OCR Cui et al. (2025)), PickScore (Kirstain et al. (2023)) and HPSv2 (Wu et al. (2023)).

5.1 EXPERIMENTAL SETUP

To make the experiments more convincing, we do experiments on two baselines, Flow-GRPO (Liu et al. (2025)) and Dance-GRPO (Xue et al. (2025)). We follow their experimental settings and only change the sampling method and the log-probability. All the experiments are conducted on 8×NVIDIA GPUs. We introduce two kinds of tasks, verifiable rewards (RLVR) and preference rewards (RLHF), to evaluate our proposed method.

RLVR Following Flow-GRPO, we use two kinds of verifiable rewards, GenEval and OCR. The GenEval is an object-focused framework to evaluate compositional image properties such as object co-occurrence, position, count, and color. The GenEval rewards are rule-based: (1) **Counting**: $r = 1 - |N_{gen} - N_{ref}|/N_{ref}$; (2) **Position/Color**: If the object count is correct, a partial reward is assigned; the remainder is granted when the predicted position or color is also correct.

The OCR reward relies on an OCR model to recognize text from the generated images and compare them with given prompts. The reward value is $r = \max(1 - N_e/N_{ref}, 0)$, where N_e is the minimum edit distance between the rendered text and target text and N_{ref} is the number of characters inside the quotation marks in the prompt.

RLHF An alternative paradigm for reward modeling is rooted in human preferences, exemplified by models like PickScore and HPSv2. The process begins with humans scoring a set of sampled images to create a preference dataset. Following this, a regression head is trained atop a foundation model, commonly the CLIP encoder, to fit these human scores. Once trained, this model serves as a direct scoring function to assess image quality.

¹The σ_t controls the noise magnitude, which cannot be very small.

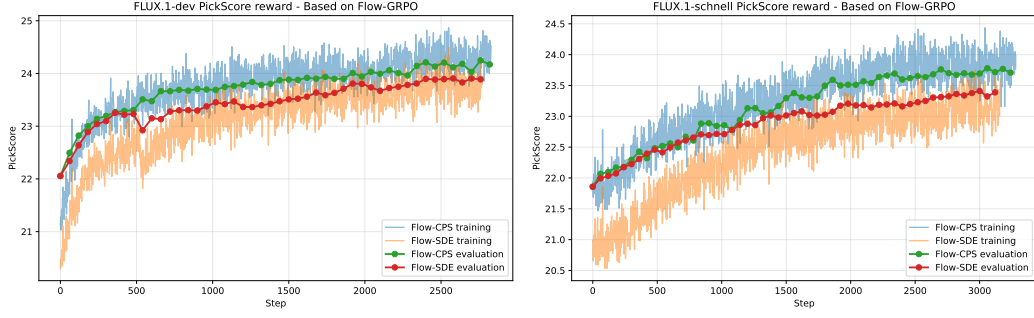


Figure 4: **Left:** PickScore optimization based on FLUX.1-dev. The sampling step number is 6 for training and 28 for evaluation. **Right:** PickScore optimization based on FLUX.1-schnell. The sampling step number is 4 for both training and evaluation. Note that there is no stochasticity during evaluation, so the rewards of the two sampling methods are the same at the beginning. For all experiments, we set $\eta = 0.9$.

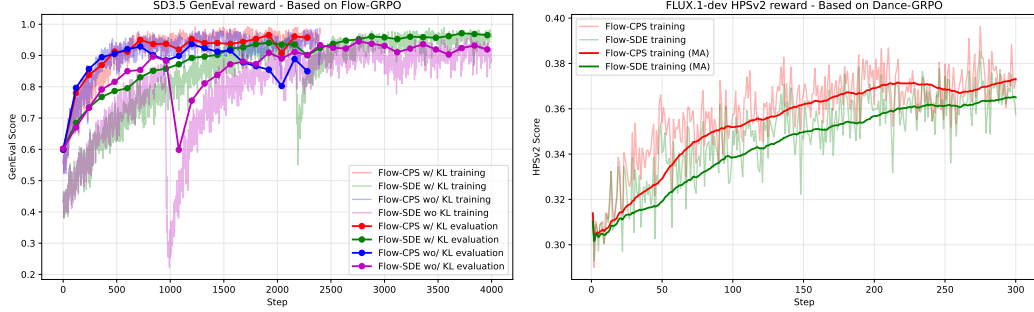


Figure 5: **Left:** GenEval optimization based on SD3.5. The sampling step number is 10 for training and 40 for evaluation. It is crucial to note that the exclusion of the KL loss resulted in significant performance degradation or model collapse for both sampling methods. We set $\eta = 0.7$ in these experiments. **Right:** HPSv2 optimization based on FLUX.1-dev. Since the codebase of Dance-GRPO does not provide online evaluation, we show the moving average of the training curves and leave the final evaluation performance in Table 3. We set $\eta = 0.7$ for our method and $\eta = 0.3$ (default value) for Dance-GRPO.

The KL loss weight, β , is a key hyperparameter in Diffusion-RL to alleviate reward hacking; we exclude it from most experiments due to its negative impact on training speed. The exception is the GenEval task, where we experimentally find that omitting the KL loss degraded performance. After careful tuning, we ultimately set $\beta = 0.001$ for our algorithm on GenEval.

5.2 CLEAN IMAGE SAMPLING

As illustrated in Figure 1, our Flow-CPS consistently generates diverse and noise-free images, even at high noise levels. Conversely, the images generated by Flow-SDE suffer from obvious noise, particularly under high noise conditions, which contributes to less reliable reward calculations. This observation is corroborated by Figure 4, which shows that Flow-CPS achieves higher rewards than Flow-SDE early in the training process. Furthermore, since the generation process is deterministic (no noise) at inference time, Flow-SDE also suffers from a more significant train-test discrepancy than Flow-CPS.

5.3 EXPERIMENTAL RESULTS

We present the results of our method on the GenEval, PickScore, HPSv2, and OCR tasks in Table 1 2 3 4, respectively. On PickScore, HPSv2 and OCR, our method consistently outperforms the two baseline methods, Flow-GRPO and Dance-GRPO. For the GenEval task, we achieve a result on par with the baselines, as the performance is already nearing saturation. However, as shown in

Table 1: GenEval Results on base model Esser et al. (2024) and base code Liu et al. (2025)

Model	Overall	Single Obj.	Two Obj.	Counting	Colors	Position	Attr. Binding
SD3.5-M (base model)	0.63	0.98	0.78	0.50	0.81	0.24	0.52
+Flow-GRPO wo/ KL	0.95	0.99	0.98	0.95	0.92	0.95	0.83
+Flow-CPS wo/ KL	0.94	0.99	0.95	0.95	0.89	0.93	0.83
+Flow-GRPO w/ KL	0.97	1.00	1.00	0.97	0.94	0.98	0.90
+Flow-CPS w/ KL	0.97	1.00	0.99	0.95	0.94	0.98	0.93

Table 2: PickScore Results

Model	PickScore
FLUX.1-schnell	21.86
+Flow-GRPO	23.39
+Flow-CPS(ours)	23.78
FLUX.1-dev	22.06
+Flow-GRPO	23.90
+Flow-CPS(ours)	24.25

Table 3: HPSv2 Results

Model	HPSv2
FLUX.1-schnell	0.304
+Dance-GRPO	0.364
+Flow-CPS(ours)	0.377

Table 4: OCR Results

Model	OCR
SD3.5-M	0.579
+Flow-GRPO	0.966
+Flow-CPS(ours)	0.975

Figure 5, our method converges to the optimal result at a faster speed, demonstrating our algorithm’s advantage.

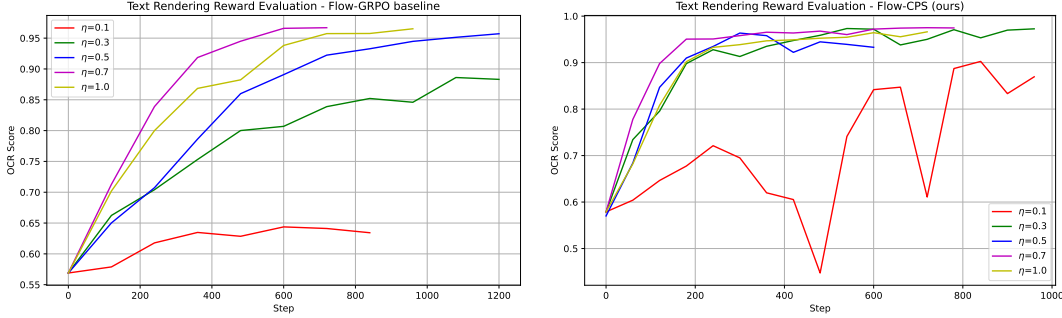


Figure 6: Text Rendering Reward comparison. Note that Flow-CPS (ours) converges faster than the Flow-GRPO baseline.

We conducted an ablation study on the hyperparameter η in Equation 12, presenting the results in Figure 6. From the figure, we can conclude that our method converges significantly faster than the Flow-GRPO baseline. Both our method and the baseline method achieve their best performance when $\eta = 0.7$, while neither method can converge properly when $\eta = 0.1$.

6 CONCLUSION

This paper introduces Coefficients-Preserving Sampling (CPS), a method that successfully addresses the image noise problem inherent in SDE-based sampling. Our theoretical analysis reveals that SDE is, in fact, a first-order Taylor approximation of CPS. Even under conditions of extremely high noise, CPS is capable of generating diverse and clean image samples. Consequently, reward optimization guided by CPS surpasses SDE-based approaches on a variety of tasks.

Nevertheless, current Flow Matching-based GRPO methods still suffer from several unresolved issues that warrant further research. Key challenges include vulnerability to reward hacking, the credit assignment problem in multi-step exploration, and an inability to optimize for the stochasticity arising from input noise.

We utilize LLMs to assist with formula derivations and writing refinement on this paper.

REFERENCES

- Josh Achiam, Steven Adler, Sandhini Agarwal, Lama Ahmad, Ilge Akkaya, Florencia Leoni Aleman, Diogo Almeida, Janko Altenschmidt, Sam Altman, Shyamal Anadkat, et al. Gpt-4 technical report. *arXiv preprint arXiv:2303.08774*, 2023.
- Kevin Black, Michael Janner, Yilun Du, Ilya Kostrikov, and Sergey Levine. Training diffusion models with reinforcement learning. *arXiv preprint arXiv:2305.13301*, 2023.
- Tom Brown, Benjamin Mann, Nick Ryder, Melanie Subbiah, Jared D Kaplan, Prafulla Dhariwal, Arvind Neelakantan, Pranav Shyam, Girish Sastry, Amanda Askell, et al. Language models are few-shot learners. *Advances in neural information processing systems*, 33:1877–1901, 2020.
- Cheng Cui, Ting Sun, Manhui Lin, Tingquan Gao, Yubo Zhang, Jiaxuan Liu, Xueqing Wang, Zelun Zhang, Changda Zhou, Hongen Liu, et al. Paddleocr 3.0 technical report. *arXiv preprint arXiv:2507.05595*, 2025.
- Hanze Dong, Wei Xiong, Deepanshu Goyal, Yihan Zhang, Winnie Chow, Rui Pan, Shizhe Diao, Jipeng Zhang, Kashun Shum, and Tong Zhang. Raft: Reward ranked finetuning for generative foundation model alignment. *arXiv preprint arXiv:2304.06767*, 2023.
- Patrick Esser, Sumith Kulal, Andreas Blattmann, Rahim Entezari, Jonas Müller, Harry Saini, Yam Levi, Dominik Lorenz, Axel Sauer, Frederic Boesel, et al. Scaling rectified flow transformers for high-resolution image synthesis. In *International conference on machine learning*, 2024.
- Leo Gao, John Schulman, and Jacob Hilton. Scaling laws for reward model overoptimization. In *International Conference on Machine Learning*, pp. 10835–10866. PMLR, 2023.
- Dhruba Ghosh, Hannaneh Hajishirzi, and Ludwig Schmidt. Geneval: An object-focused framework for evaluating text-to-image alignment. *Advances in Neural Information Processing Systems*, 36: 52132–52152, 2023.
- Jack Hessel, Ari Holtzman, Maxwell Forbes, Ronan Le Bras, and Yejin Choi. Clipscore: A reference-free evaluation metric for image captioning. *arXiv preprint arXiv:2104.08718*, 2021.
- Jonathan Ho, Ajay Jain, and Pieter Abbeel. Denoising diffusion probabilistic models. *Advances in neural information processing systems*, 33:6840–6851, 2020.
- Yudong Jiang, Baohan Xu, Siqian Yang, Mingyu Yin, Jing Liu, Chao Xu, Siqi Wang, Yidi Wu, Bingwen Zhu, Xinwen Zhang, et al. Anisora: Exploring the frontiers of animation video generation in the sora era. *arXiv preprint arXiv:2412.10255*, 2024.
- Tero Karras, Miika Aittala, Timo Aila, and Samuli Laine. Elucidating the design space of diffusion-based generative models. *Advances in neural information processing systems*, 35:26565–26577, 2022.
- Yuval Kirstain, Adam Polyak, Uriel Singer, Shahbuland Matiana, Joe Penna, and Omer Levy. Pick-a-pic: An open dataset of user preferences for text-to-image generation. *Advances in neural information processing systems*, 36:36652–36663, 2023.
- Yaron Lipman, Ricky TQ Chen, Heli Ben-Hamu, Maximilian Nickel, and Matt Le. Flow matching for generative modeling. *arXiv preprint arXiv:2210.02747*, 2022.
- Jie Liu, Gongye Liu, Jiajun Liang, Yangguang Li, Jiaheng Liu, Xintao Wang, Pengfei Wan, Di Zhang, and Wanli Ouyang. Flow-grpo: Training flow matching models via online rl. *arXiv preprint arXiv:2505.05470*, 2025.
- Xingchao Liu, Chengyue Gong, and Qiang Liu. Flow straight and fast: Learning to generate and transfer data with rectified flow. *arXiv preprint arXiv:2209.03003*, 2022.
- Cheng Lu, Yuhao Zhou, Fan Bao, Jianfei Chen, Chongxuan Li, and Jun Zhu. Dpm-solver: A fast ode solver for diffusion probabilistic model sampling in around 10 steps. *Advances in neural information processing systems*, 35:5775–5787, 2022.

- Cheng Lu, Yuhao Zhou, Fan Bao, Jianfei Chen, Chongxuan Li, and Jun Zhu. Dpm-solver++: Fast solver for guided sampling of diffusion probabilistic models. *Machine Intelligence Research*, pp. 1–22, 2025.
- Zichen Miao, Jiang Wang, Ze Wang, Zhengyuan Yang, Lijuan Wang, Qiang Qiu, and Zicheng Liu. Training diffusion models towards diverse image generation with reinforcement learning. In *Proceedings of the IEEE/CVF Conference on Computer Vision and Pattern Recognition*, pp. 10844–10853, 2024.
- Long Ouyang, Jeffrey Wu, Xu Jiang, Diogo Almeida, Carroll Wainwright, Pamela Mishkin, Chong Zhang, Sandhini Agarwal, Katarina Slama, Alex Ray, et al. Training language models to follow instructions with human feedback. *Advances in neural information processing systems*, 35: 27730–27744, 2022.
- Rafael Rafailov, Archit Sharma, Eric Mitchell, Christopher D Manning, Stefano Ermon, and Chelsea Finn. Direct preference optimization: Your language model is secretly a reward model. *Advances in neural information processing systems*, 36:53728–53741, 2023.
- John Schulman, Filip Wolski, Prafulla Dhariwal, Alec Radford, and Oleg Klimov. Proximal policy optimization algorithms. *arXiv preprint arXiv:1707.06347*, 2017.
- Zhihong Shao, Peiyi Wang, Qihao Zhu, Runxin Xu, Junxiao Song, Xiao Bi, Haowei Zhang, Mingchuan Zhang, YK Li, Yang Wu, et al. Deepseekmath: Pushing the limits of mathematical reasoning in open language models. *arXiv preprint arXiv:2402.03300*, 2024.
- Jiaming Song, Chenlin Meng, and Stefano Ermon. Denoising diffusion implicit models. In *International Conference on Learning Representations*, 2021a.
- Yang Song, Jascha Sohl-Dickstein, Diederik P Kingma, Abhishek Kumar, Stefano Ermon, and Ben Poole. Score-based generative modeling through stochastic differential equations. In *International Conference on Learning Representations*, 2021b.
- Yang Song, Prafulla Dhariwal, Mark Chen, and Ilya Sutskever. Consistency models. In *International Conference on Machine Learning*, pp. 32211–32252. PMLR, 2023.
- Bram Wallace, Meihua Dang, Rafael Rafailov, Linqi Zhou, Aaron Lou, Senthil Purushwalkam, Stefano Ermon, Caiming Xiong, Shafiq Joty, and Nikhil Naik. Diffusion model alignment using direct preference optimization. In *Proceedings of the IEEE/CVF Conference on Computer Vision and Pattern Recognition*, pp. 8228–8238, 2024.
- Feng Wang. Understanding diffusion and flow matching with zero derivation, 2024. URL <https://zhuanlan.zhihu.com/p/11228697012>.
- Xiaoshi Wu, Yiming Hao, Keqiang Sun, Yixiong Chen, Feng Zhu, Rui Zhao, and Hongsheng Li. Human preference score v2: A solid benchmark for evaluating human preferences of text-to-image synthesis. *arXiv preprint arXiv:2306.09341*, 2023.
- Jiazheng Xu, Xiao Liu, Yuchen Wu, Yuxuan Tong, Qinkai Li, Ming Ding, Jie Tang, and Yuxiao Dong. Imagereward: Learning and evaluating human preferences for text-to-image generation. *Advances in Neural Information Processing Systems*, 36:15903–15935, 2023.
- Zeyue Xue, Jie Wu, Yu Gao, Fangyuan Kong, Lingting Zhu, Mengzhao Chen, Zhiheng Liu, Wei Liu, Qiushan Guo, Weilin Huang, et al. Dancegrp: Unleashing grp on visual generation. *arXiv preprint arXiv:2505.07818*, 2025.
- Kai Yang, Jian Tao, Jiafei Lyu, Chunjiang Ge, Jiabin Chen, Weihang Shen, Xiaolong Zhu, and Xiu Li. Using human feedback to fine-tune diffusion models without any reward model. In *Proceedings of the IEEE/CVF Conference on Computer Vision and Pattern Recognition*, pp. 8941–8951, 2024.
- Tianwei Yin, Michaël Gharbi, Richard Zhang, Eli Shechtman, Fredo Durand, William T Freeman, and Taesung Park. One-step diffusion with distribution matching distillation. In *Proceedings of the IEEE/CVF conference on computer vision and pattern recognition*, pp. 6613–6623, 2024.

Hanyang Zhao, Haoxian Chen, Ji Zhang, David D Yao, and Wenpin Tang. Score as action: Fine-tuning diffusion generative models by continuous-time reinforcement learning. *arXiv preprint arXiv:2502.01819*, 2025.

Wenliang Zhao, Lujia Bai, Yongming Rao, Jie Zhou, and Jiwen Lu. Unipc: A unified predictor-corrector framework for fast sampling of diffusion models. *Advances in Neural Information Processing Systems*, 36:49842–49869, 2023.

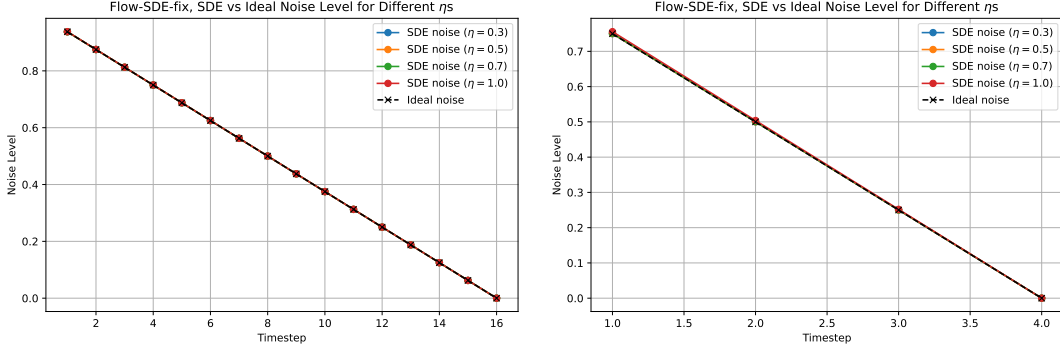


Figure 7: The ideal and SDE noise level for Equation 18.

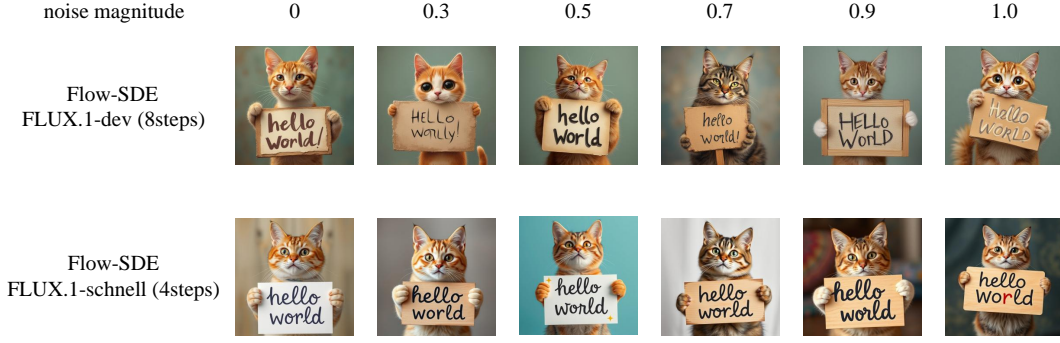


Figure 8: Image sampled by Equation 18. There is no obvious noise on these images.

A VP-SDE IS AN APPROXIMATION OF DDPM

Similar to Theorem 1, VP-SDE (Song et al. (2021b)) can also be seen as a first-order Taylor approximation of DDPM. In the VP-SDE, the forward process is,

$$\begin{aligned}
 \mathbf{x}(t + \Delta t) &= \sqrt{1 - \beta(t + \Delta t)\Delta t} \mathbf{x}(t) + \sqrt{\beta(t + \Delta t)\Delta t} \mathbf{z}(t) \\
 &\approx \mathbf{x}(t) - \frac{1}{2}\beta(t + \Delta t)\Delta t \mathbf{x}(t) + \sqrt{\beta(t + \Delta t)\Delta t} \mathbf{z}(t) \\
 &\approx \mathbf{x}(t) - \frac{1}{2}\beta(t)\Delta t \mathbf{x}(t) + \sqrt{\beta(t)\Delta t} \mathbf{z}(t),
 \end{aligned} \tag{17}$$

where the approximate equality holds when $\Delta t \ll 1$. Similar to formula 16, it uses Taylor expansion and omits the second and higher order terms.

For the VP SDE backward process, please refer to Appendix E of Song et al. (2021b), which also uses Taylor expansion and omits high-order terms in the derivation. Song et al. (2021b) claimed that the ancestral sampler of DDPM is essentially a discretization of the reverse-time SDE. Conversely, if a pre-trained DDPM is given, we can also say that the reverse process of the VP-SDE is a continuous approximation of DDPM ancestral sampling.

B AN ALTERNATIVE FOR THE NUMERICAL PROBLEM

In section 4.4, we mentioned that Flow-SDE has a numerical problem because of the $\frac{1}{t}$ term. One possible patch would be setting $\sigma_t = \eta(t - \Delta t)$, then the Flow-SDE becomes,

$$\begin{aligned}
 \mathbf{x}_{t-\Delta t} &\approx (1 - (t - \Delta t)) \hat{\mathbf{x}}_0 + \left(t - \Delta t - \frac{\eta^2}{2}(t - \Delta t)\Delta t \right) \hat{\mathbf{x}}_1 + \eta(t - \Delta t)\sqrt{\Delta t}\epsilon \\
 &= \mathbf{x}_t - \hat{\mathbf{v}}_\theta(\mathbf{x}_t, t)\Delta t - \frac{\eta^2}{2}(t - \Delta t)\Delta t \hat{\mathbf{x}}_1 + \eta(t - \Delta t)\sqrt{\Delta t}\epsilon \\
 &\approx \mathbf{x}_t - \hat{\mathbf{v}}_\theta(\mathbf{x}_t, t)\Delta t - \frac{\eta^2}{2}t\hat{\mathbf{x}}_1\Delta t + \eta t\sqrt{\Delta t}\epsilon.
 \end{aligned} \tag{18}$$

In the limit of $\Delta t \rightarrow 0$, this equation converges to the following SDE,

$$d\mathbf{x}_t = \hat{\mathbf{v}}_\theta(\mathbf{x}_t, t)dt + \frac{\eta^2}{2}t\hat{\mathbf{x}}_1(\mathbf{x}_t, t)dt + \eta t d\mathbf{w} \tag{19}$$

Even though this formula still cannot satisfy the requirements of CPS, it has a smaller error than the original Flow-SDE. We show the noise level in Figure 7 and sampled images in Figure 8. It would be useful when the characteristics of the SDE are to be exploited.